



Electrostatic Potentials at Solid/Liquid Interfaces*

Nikola Kallay,^{a,**} Tajana Preočanin,^a Davor Kovačević,^a
 Johannes Lützenkirchen,^b and Emil Chibowski^c

^aLaboratory of Physical Chemistry, Department of Chemistry, Faculty of Science, University of Zagreb,
 Horvatovac 102a, 10000 Zagreb, Croatia

^bInstitut für Nukleare Entsorgung, Karlsruher Institut für Technologie, Postfach 3640, 76021 Karlsruhe, Germany

^cPhysical Chemistry Department, Faculty of Chemistry, Maria Curie-Skłodowska University,
 pl. Marii Curie-Skłodowskiej 3, 20.031 Lublin, Poland

RECEIVED NOVEMBER 23, 2009; REVISED FEBRUARY 4, 2010; ACCEPTED FEBRUARY 12, 2010

Abstract. This review deals with electrostatic potentials within solid/electrolyte interfaces. The electrostatic potentials of several planes are defined and discussed: the inner surface potential affecting the state of charged surface species due to interactions with potential determining ions (Ψ_0), the potential affecting the state of associated counterions (Ψ_β), the potential at the onset of diffuse layer (Ψ_d) and the electrokinetic potential (ζ). The relevance of zero values of these potentials is also discussed and the corresponding points of zero charge are defined. Experimental methods for the measurement of the interfacial potentials are presented. The relations between potentials and surface charges are given on the basis of the Surface Complexation model. Some experimental findings are provided.

Keywords: electrostatic potential, solid/electrolyte interface, Surface Complexation model, surface charge

INTRODUCTION

Ionic interactions at the solid/liquid interface result in accumulation of charge at the interface and in development of an electrostatic potential. Electrostatic potentials are directly related to binding and distribution of charged ionic species at the interface. One may conclude that the interfacial electrostatic potential is determined by the charge distribution which is in turn influenced by the electrostatic potential affecting the state of charged ionic species through their interfacial activity coefficients. This mutual dependency is the subject of numerous publications.^{1–4} The present review article concerns electrostatic potentials within the electrical interfacial layer (EIL), their evaluation from the interfacial equilibrium and their more or less direct measurements.

Within the interfacial layer the potential decreases from the solid surface to the bulk of the solution (Figure 1) which is commonly taken as the reference point characterized by the zero value of the electrostatic potential.^{5–7} In order to analyze interfacial potentials one should simplify the reality by assuming a certain model with several layers at the interface divided by characteristic planes. For that purpose we shall use the General Model

of EIL (GM-EIL) of a metal oxide in aqueous solution of 1:1 simple electrolyte. The GM-EIL is described in Figure 1. Within the solid phase the potential is assumed to be constant and equal to the inner surface potential Ψ_0 corresponding to the 0-plane that divides the solid from the liquid phase. The surface charge density of this plane, σ_0 , is determined by interaction of potential determining ions with the active surface sites (H^+ and OH^- ions in the case of metal oxides). The charge at the 0-plane is partially compensated by association of charged surface groups with counterions of opposite sign of charge. These associated counterions are located at the β -plane. The layer between these two planes may be called inner Helmholtz layer, the boundary of which are the 0-plane characterized by the potential Ψ_0 and the β -plane symbolized by the potential Ψ_β . The onset of the diffuse layer which extends to the bulk of the solution is at the d-plane with potential Ψ_d . The layer between the β -plane and the d-plane may be called outer Helmholtz layer. Within the diffuse layer the electrokinetic slip plane (e-plane) is located dividing the mobile from the stagnant liquid at the interface and is characterized by the electrokinetic ζ -potential.

Accordingly, four different electrostatic potentials characterize the EIL:

* Presented at the Discussion Meeting *Surface Reactions and EIL, Experiments and Models towards a Common Basis*, Opatija, October, 2007.

** Author to whom correspondence should be addressed. (E-mail: nkallay@chem.pmf.hr)

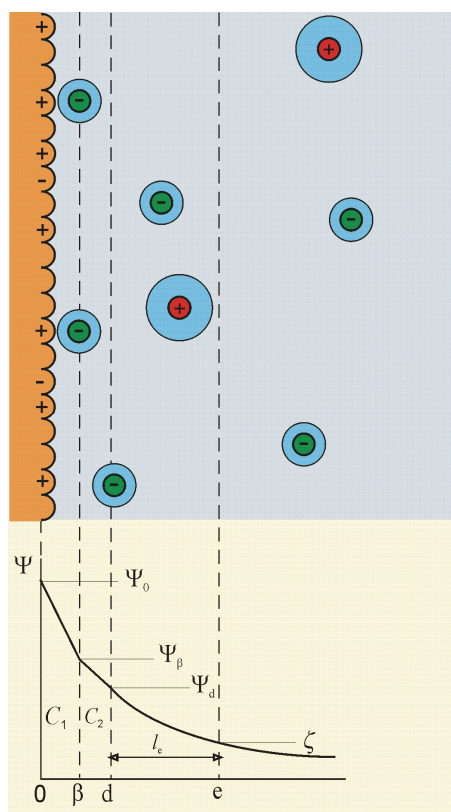


Figure 1. General Model of the Electrical Interfacial Layer (GM-EIL). Reproduced with permission from *Croatia Chemica Acta*.⁸

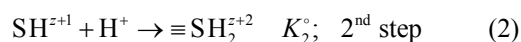
- the inner surface potential Ψ_0 affecting the state of surface charges developed by interactions of active surface groups with potential determining ions
- the outer surface potential Ψ_β affecting the state of associated counterions
- the potential at the onset of diffuse layer Ψ_d affecting ion distribution (charge density) within the diffuse layer.
- the electrokinetic ζ -potential determined by Ψ_d , ion distribution within diffuse layer and the slip-plane separation l_e .

Some of the above mentioned potentials can be determined experimentally. The (inner) surface potential Ψ_0 can be obtained by means of Ion Sensitive Field Effect Transistors⁹⁻¹⁶ or by means of Single Crystal Electrodes.¹⁷⁻²⁴ The electrokinetic ζ -potential can be measured by means of various electrokinetic methods.^{5,25} The potential at the onset of the diffuse layer Ψ_d can be obtained from Atomic Force Microscopy data.²⁶

INTERFACIAL EQUILIBRIUM

Electrostatic potentials within the interfacial layer are related to interfacial equilibrium, so that they may be

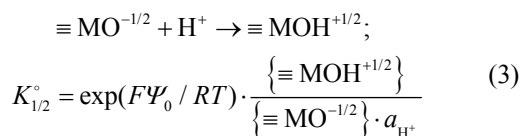
evaluated from adsorption data. In order to demonstrate the procedure the Site Binding or Surface Complexation Model (SCM) will be applied. According to SCM theory several reactions may take place at the interface. The charging reactions could be represented by binding of potential determining ions to the active surface sites. In the case of metal oxides potential determining ions are H^+ ions (and/or OH^- ions). Generally, one can write the reaction Equation as binding of H^+ ions to active sites $\equiv S^z$ of charge number z . The protonation of active surface sites may proceed in one or two steps



where K_1° and K_2° denote the thermodynamic equilibrium constants of the corresponding surface reactions.

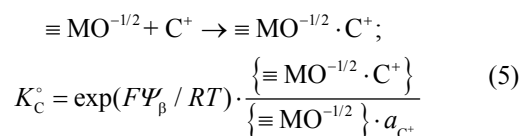
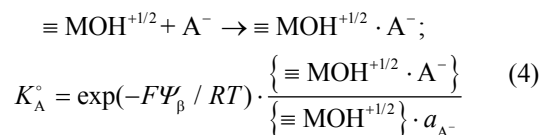
One-step protonation (1-pK concept)

In the case of one step protonation (1-pK concept²⁷⁻²⁹) the original charge number z may be e.g. $-1/2$ so that $\equiv S^z$ is $\equiv MO^{-1/2}$. Here M denotes a metal atom. Accordingly,



where a denotes the activity in the bulk of the solution, $K_{1/2}^\circ$ is the thermodynamic equilibrium constant of the corresponding surface reaction, and Ψ_0 is the electrostatic surface potential (inner surface potential) affecting the state of charged surface groups $\equiv MO^{-1/2}$ and $\equiv MOH^{+1/2}$. Curly brackets denote surface concentrations (amount of surface species per surface area) which are proportional to the activities of interfacial species. The exponential term in Equation (3) represents the activity coefficients of charged surface species.³⁰

The effective (net) surface charge is reduced by association of anions A^- and cations C^+ from the bulk of solution with oppositely charged surface sites



where K_A° and K_C° are thermodynamic equilibrium constants for association of counterions at the interface. Other symbols have their usual meaning.

The inner surface potential Ψ_0 in the case of the 1-pK concept is, according to Equation (3), given by

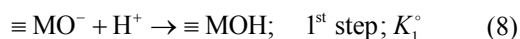
$$\Psi_0 = \frac{RT \ln 10}{F} \log K_{1/2}^\circ - \frac{RT \ln 10}{F} \log \left(\frac{\{\equiv \text{MOH}^{+1/2}\}}{\{\equiv \text{MO}^{-1/2}\}} \right) - \frac{RT \ln 10}{F} \text{pH} \quad (6)$$

Total density of surface sites is given by

$$\Gamma_{\text{tot}} = \{\equiv \text{MOH}^{+1/2}\} + \{\equiv \text{MOH}^{+1/2} \cdot \text{A}^-\} + \{\equiv \text{MO}^{-1/2}\} + \{\equiv \text{MO}^{-1/2} \cdot \text{C}^+\} \quad (7)$$

Two-step protonation (2-pK concept)

In the case of two-step protonation (2-pK concept^{31,32}) the original charge number z is -1 so that $\equiv \text{S}^z$ is $\equiv \text{MO}^-$. Accordingly,



According to the original 2-pK concept, the reaction Equation (8) could be written in the opposite direction, *i.e.* as deprotonation of amphoteric $\equiv \text{MOH}$ groups. By introducing the interfacial activity coefficients the thermodynamic equilibrium constants of the corresponding surface reactions, K_1° and K_2° are

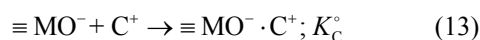
$$K_1^\circ = \exp(\Psi_0 F / RT) \cdot \frac{\{\equiv \text{MOH}\}}{\{\equiv \text{MO}^-\} \cdot a_{\text{H}^+}} \quad (10)$$

$$K_2^\circ = \exp(\Psi_0 F / RT) \cdot \frac{\{\equiv \text{MOH}_2^+\}}{\{\equiv \text{MOH}\} \cdot a_{\text{H}^+}} \quad (11)$$

where Ψ_0 is the electrostatic potential affecting the state of charged surface groups $\equiv \text{MOH}_2^+$ and $\equiv \text{MO}^-$. The interfacial thermodynamic equilibrium constants K_1° and K_2° were formerly called “intrinsic equilibrium constants”. The concept of “intrinsic equilibrium constant” assumes two hypothetical steps. The first one is distribution of potential determining ions between bulk of the solution and the interface, as quantitatively described by the Boltzmann statistics. The second process is binding of potential determining ions at the interface with surface sites and is characterized by the “intrinsic equilibrium constant”. Note that the equilibrium constant K_1° for the first protonation step is

equal to the reciprocal value of the deprotonation equilibrium constant.

Within the two-step mechanism, the effective (net) surface charge is reduced by association of anions A^- and cations C^+ with oppositely charged surface groups by



where the corresponding thermodynamic equilibrium constants K_A° and K_C° are

$$K_A^\circ = \exp(-\Psi_\beta F / RT) \cdot \frac{\{\equiv \text{MOH}_2^+ \cdot \text{A}^-\}}{\{\equiv \text{MOH}_2^+\} \cdot a_{\text{A}^-}} \quad (14)$$

$$K_C^\circ = \exp(\Psi_\beta F / RT) \cdot \frac{\{\equiv \text{MO}^- \cdot \text{C}^+\}}{\{\equiv \text{MO}^-\} \cdot a_{\text{C}^+}} \quad (15)$$

Again, Ψ_β is the electrostatic potential affecting the state of associated counterions.

Total density of surface sites is given by

$$\Gamma_{\text{tot}} = \{\equiv \text{MOH}\} + \{\equiv \text{MOH}_2^+\} + \{\equiv \text{MOH}_2^+ \cdot \text{A}^-\} + \{\equiv \text{MO}^-\} + \{\equiv \text{MO}^- \cdot \text{C}^+\} \quad (16)$$

According to the two-step protonation mechanism (2-pK concept) of the Surface Complexation Model (Equations (14) and (15)), the inner surface potential Ψ_0 is given by

$$\Psi_0 = \frac{RT \ln 10}{F} \log K_1^\circ - \frac{RT \ln 10}{F} \lg \left(\frac{\{\equiv \text{MOH}\}}{\{\equiv \text{MO}^-\}} \right) - \frac{RT \ln 10}{F} \text{pH} \quad (17)$$

$$\Psi_0 = \frac{RT \ln 10}{F} \log K_2^\circ - \frac{RT \ln 10}{F} \lg \left(\frac{\{\equiv \text{MOH}_2^+\}}{\{\equiv \text{MOH}\}} \right) - \frac{RT \ln 10}{F} \text{pH} \quad (18)$$

Summation of Equations (17) and (18) leads to

$$\Psi_0 = \frac{RT \ln 10}{2F} \left[\log(K_1^\circ \cdot K_2^\circ) - \lg \left(\frac{\{\equiv \text{MOH}_2^+\}}{\{\equiv \text{MO}^-\}} \right) - 2 \text{pH} \right] \quad (19)$$

By introducing the electroneutrality point pH_{eln} (also called pristine point of zero charge^{20,33-36} pH_{ppzc})

$$\text{pH}_{\text{eln}} = \frac{1}{2} \log(K_1^\circ \cdot K_2^\circ) \quad (20)$$

one obtains

$$\Psi_0 = \frac{RT \ln 10}{2F} \log \left(\frac{\{\equiv \text{MO}^-\}}{\{\equiv \text{MOH}_2^+\}} \right) - \frac{RT \ln 10}{F} (\text{pH} - \text{pH}_{\text{eln}}) \quad (21)$$

Physical meaning of the electroneutrality point will be discussed in the next section of this article. The value of pH_{eln} can be experimentally obtained at sufficiently low ionic strength where the electroneutrality point pH_{eln} coincides with the point of zero charge (point of zero net proton charge) pH_{pzc} ($\sigma_0 = 0$), the isoelectric point pH_{iep} ($\mu = 0$, corresponding in most cases to $\zeta = 0$, where μ is the electrokinetic mobility, *i.e.* the directly measured quantity) and the point of zero surface potential pH_{pzp} ($\Psi_0 = 0$).

INTERFACIAL POTENTIALS

Surface Charge Densities and Interfacial Potentials

Surface charge densities in different planes are related to corresponding surface concentrations of charged ionic species. In the case of the two-step protonation mechanism (2-pK concept) the surface charge density of the 0-plane is given by

$$\sigma_0 = F \cdot \left(\{\equiv \text{MOH}_2^+\} + \{\equiv \text{MOH}_2^+ \cdot \text{A}^-\} - \{\equiv \text{MO}^-\} - \{\equiv \text{MO}^- \cdot \text{C}^+\} \right) \quad (22)$$

and for the β -plane

$$\sigma_\beta = F \cdot \left(\{\equiv \text{MO}^- \cdot \text{C}^+\} - \{\equiv \text{MOH}_2^+ \cdot \text{A}^-\} \right) \quad (23)$$

The effective (net) surface charge density σ_s is equal in magnitude and opposite in sign to the surface charge density of the diffuse layer σ_d

$$\sigma_s = -\sigma_d = \sigma_0 + \sigma_\beta = F \cdot \left(\{\equiv \text{MOH}_2^+\} - \{\equiv \text{MO}^-\} \right) \quad (24)$$

The relationships between surface charge densities and interfacial electrostatic potentials are often based on the concept of condensers of constant capacitance C (expressed per surface area) as

$$C_1 = \frac{\sigma_0}{\Psi_0 - \Psi_\beta} \quad (25)$$

$$C_2 = \frac{\sigma_s}{\Psi_\beta - \Psi_d} \quad (26)$$

and by the Gouy-Chapman theory. For flat surfaces

$$\sigma_d = -\sigma_s = -\sqrt{8RT\varepsilon I_c} \sinh(-F\Psi_d / RT) \quad (27)$$

or

$$\Psi_d = \frac{2RT}{F} \text{ar sinh} \frac{\sigma_d}{\sqrt{8RT\varepsilon I_c}} \quad (28)$$

where ε ($\varepsilon = \varepsilon_0 \cdot \varepsilon_r$) is permittivity. I_c is the ionic strength determined by the concentrations (c) and the respective charge numbers (z) of all ions present in the system (in the bulk solution) according to

$$I_c = \frac{1}{2} \sum_i c_i \cdot z_i^2 \quad (29)$$

When the Gouy-Chapman theory is applied the common practice is to use the permittivity of the bulk of the solution.⁶ However, it is known³⁷ that the value of the permittivity of water near the surfaces is lowered, $6 < \varepsilon_r < 80$. The value increases with the distance, and decreases with the surface charge.³⁹ A self-consistent calculation of both the effective bulk solution ionic strength and the corresponding relative permittivity should take into account the amount of electrolyte ions adsorbed. The fraction of those adsorbed ions is usually assumed to be rather low.

According to the Gouy-Chapman theory for flat surfaces the electrokinetic potential ζ is related to the potential at the onset of diffuse layer Ψ_d by

$$\Psi_d = \frac{2RT}{F} \ln \left(\frac{\exp(-\kappa l_e) + \tanh(F\zeta / 4RT)}{\exp(-\kappa l_e) - \tanh(F\zeta / 4RT)} \right) \quad (30)$$

or

$$\ln \tanh \frac{F\zeta}{4RT} = \ln \tanh \left(\frac{F\Psi_d}{4RT} \right) - \kappa l_e \quad (31)$$

where κ is the Debye-Hückel parameter given by

$$\kappa = \sqrt{\frac{2I_c F^2}{\varepsilon RT}} \quad (32)$$

For relatively low potentials Equation (31) could be reduced to

$$\zeta = \Psi_d e^{-\kappa l_e} \quad (33)$$

For spherical particles of radius r and for 1:1 electrolytes, the following equation is an analytical approximation for sufficiently low potentials

$$\Psi_d = -\frac{2Fl_c}{\kappa} \left[2\sinh\left(\frac{\sigma_d}{2}\right) + \frac{4\tanh(\sigma_d/4)}{\kappa r} \right] \quad (34)$$

Potentiometric acid-base titration and mass titration of a metal oxide suspension provides dependency of σ_0 on pH. The interpretation of these data (by means of Equations (10,11,22–28)) yields equilibrium parameters (equilibrium constants and capacitances), as well as the dependency of interfacial potentials on pH.

Relationships between interfacial potentials

According to Equations (25,26,30) and GM-EIL (Figure 1), the magnitude of the electrostatic potential decreases from the solid surface towards the bulk of the solution

$$|\Psi_0| > |\Psi_\beta| > |\Psi_d| > |\zeta| \quad (35)$$

The general model of electrical interfacial layer (GM-EIL) may be simplified to the Basic Stern Model⁴² (BSM) or to the Triple Layer Model (TLM) as originally proposed by Leckie and coworkers.³¹

According to the TLM there is a potential drop from 0- to β -plane, and from β -plane to d-plane, which means that $0 < C_1 \ll \infty$ and also $0 < C_2 \ll \infty$. The simplification lies in the assumption that the Ψ_d potential is approximately equal to electrokinetic ζ -potential, which corresponds to a zero value of the slip-plane separation ($l_c = 0$) so that

$$|\Psi_0| > |\Psi_\beta| > |\Psi_d| = |\zeta|; \text{ TLM} \quad (36)$$

According to the BSM the potential drop between β - and d-plane is neglected as they are assumed to be identical, which corresponds to $0 < C_1 \ll \infty$, and $C_2 = \infty$. However, the potential drop between d-plane and electrokinetic slip plane cannot be neglected if zeta-potentials are to be described, which corresponds to $l_c > 0$. Accordingly,

$$|\Psi_0| > |\Psi_\beta| = |\Psi_d| > |\zeta|; \text{ BSM} \quad (37)$$

Both approximations satisfy well the established requirement that the magnitude of the inner surface potential Ψ_0 should be higher with respect to the potential to which associated counterions are exposed Ψ_β , and that electrokinetic ζ -potential should be lower in magnitude than the Ψ_β potential.

$$|\Psi_0| > |\Psi_\beta| > |\zeta| \quad (38)$$

The inner surface potential Ψ_0

The inner surface potential, or simply just surface potential, Ψ_0 , is the electrostatic potential at the solid plane

exposed to the liquid medium. Since this potential markedly affects the state of charged species bound directly to the surface Equations (10,11), it plays a dominant role in equilibration of the interfacial layer. The expressions for the inner surface potential depend on the assumed mechanism of surface protonation. However, they may be reduced to the common expression if the general Equation for protonation of any kind of surface sites is considered (Equation (1))

$$\Psi_0 = \frac{RT \ln 10}{F} \log K_1^\circ - \frac{RT \ln 10}{F} \log \left(\frac{\{ \equiv \text{SH}^{z+1} \}}{\{ \equiv \text{S}^z \}} \right) - \frac{RT \ln 10}{F} \text{pH} \quad (39)$$

The function $\Psi_0(\text{pH})$ is often approximated as a linear function. The last term in Equation (39) suggests the Nernstian slope of the $\Psi_0(\text{pH})$ function, but the second term on the right hand side, determined by the ratio of free (more) positive and free (more) negative surface groups, causes reduction of the slope and possible deviation from linearity.

Measurements of the inner surface potential Ψ_0 provide important information on the equilibrium at the interfacial layer. Deviation from the Nernstian slope yields information on the ratio of surface concentrations of (more) positively to (more) negatively charged surface groups. Since the measurements of the surface charge, but also electrokinetic data, provide the charge, *i.e.* difference in concentrations of charged groups at the surface, one may combine these data and characterize the interface in a more comprehensive way.

The Ion Sensitive Field Effect Transistors (ISFET) were successfully used for SiO_2 surfaces^{9,10} and Al_2O_3 surfaces.¹¹ Another route to measure Ψ_0 is to prepare a metal oxide electrode. First attempts using the metal wires covered with metal oxides did not provide reliable data (iridium oxide,¹² zirconium oxide,¹³ titanium oxide,¹⁴ hematite¹⁵ and palladium oxide¹⁶). Due to the porosity of the oxide layer, the solution could have direct contact with the metal wire so that such an electrode behaves as the electrode of the second kind. The problem of the porosity was for the first time solved by construction of the ice electrode.¹⁷ On the basis of this experience, the Single Crystal Electrodes (SCrE) of different metal oxides were constructed,⁸ as presented in Figure 2.

The inner surface potential Ψ_0 is a measurable quantity. It is known that single crystal electrodes were used in electrolysis. For example, they were applied for electrochemical photolysis of water (n-type TiO_2 crystal, n-type $\alpha\text{-Fe}_2\text{O}_3$ crystal). The first measurement of the equilibrium surface potential by single crystal electrode was performed with ice electrode and published¹⁷

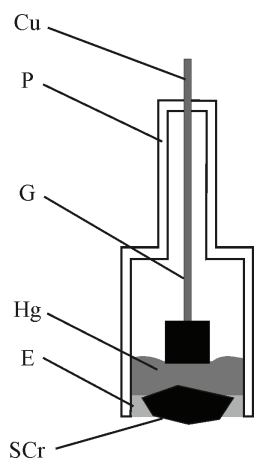


Figure 2. Single Crystal Electrode for surface potential measurements: (SCr – metal oxide single crystal, Hg – mercury, G – graphite, Cu – copper wire, P – plexiglas, E – epoxy resin). Reproduced with permission from *Croatia Chemica Acta*.⁸

in 2000, while the second report with hematite single crystal electrode appeared¹⁹ in 2005.

Measurements with the Single Crystal Electrodes meet several problems, such as resistance of the crystal, reversibility of interfacial reactions, hysteresis and evaluation of the surface potentials from the measured values of the relative electrode potentials.

Resistance of the electrode

In principle one should use a potentiometer with internal impedance (resistance) that is sufficiently high with respect to the resistance of the SCrE. The resistance of the reference electrode is not a problem. In most of the cases the resistance of the SCrE is lower than few gigohms so that a commercial pH-meter satisfies the requirement. A simple test is based on the reasonable assumption that a pH meter produces correct values of the potential of the glass electrode. Therefore, one should measure the potential of the glass electrode and of SCrE in the same solution, but separately. The readings would be different. In the second step one connects the glass electrode and SCrE in parallel and measures the potential difference for the same solution with respect to the same reference electrode as used in the first step. If the reading is close to the previous reading for SCrE, the internal resistance of SCrE is lower than that of the glass electrode and one may use the pH meter for measurements of the electrode potential of SCrE. If the reading is close to that previously obtained for the glass electrode, the resistance of the SCrE is too high and the commercial pH meter cannot be used. In such a case one should use potentiometers of higher input impedance. Instruments of internal impedance of $10^{15} \Omega$ are commercially available.

Reversibility and interfacial equilibrium

In the case of an equilibrated interface the rate of ionic

adsorption is equal to the rate of ionic desorption. Even when using a high impedance instrument a current still passes through the interface. The rates of binding and release of p.d.i. are not equal and one cannot be sure that measured values correspond to equilibrium. The equilibrium condition may be in principle achieved by applying the Poggendorf compensation method. However, despite the high sensitivity of the galvanometer, this method cannot be applied for high resistance SCrEs. For that purpose the original Poggendorf compensation method was modified by introducing the pH-meter as the indicator of the compensation. It was shown that such a set up may be used for electrodes having resistance even as high as that of the pH-meter. For details see Reference 45. This approach enables an additional test. The introduced potential supplied from the bridge may be higher or lower than the electromotive force (*i.e.* electromotivity⁴⁶) of the examined cell (SCrE-reference electrode) so that a current passes through the interface. The direction may also be changed and the state at the interface is then shifted from its equilibrium state. If the SCrE electrode potential remains the same, *i.e.* if the disturbance does not have any effect, the system is sufficiently reversible and one may use a pH-meter to obtain values that correspond to interfacial equilibrium.

Hysteresis

In the case of slow interfacial equilibration a relatively stable reading is usually reached after few minutes, but the obtained values still do not correspond to the equilibrium. Therefore, it is strongly advisable to perform titrations in both directions and to examine possible hysteresis. Indeed such a hysteresis was observed with a hematite single crystal electrode.²¹ The problem should then be solved by prolonged equilibration time, but it was also shown that application of ultrasound makes interfacial equilibration significantly faster.

Conversion of electrode potentials to surface potentials

The measured potential difference or electrode potential of SCrE is the sum of all potential differences in the measuring circuit (from contact potentials to the potential difference at the reference electrode). The only one that depends on the solution composition (for metal oxides the major issue is here the proton concentration, *i.e.* pH) is the surface potential, or more precisely the potential difference between the bulk of the crystal and the bulk of the solution. Therefore, the measured electrode potential of the SCrE E is equal to the relative value of the surface potential Ψ_0 . Since the measured electromotivities are the sum of all potential differences in the circuit, one needs to set the zero value of the surface potential Ψ_0 , *i.e.*, to know the point of zero potential pH_{pzp} . It was assumed that pH_{pzp} is close to pH_{iep} and so the isoelectric point was used to set the zero

value of the $\Psi_0(\text{pH})$ function.^{20,47} This procedure is correct at relatively low ionic strengths, especially for electrolytes with cations and anions of similar surface association affinities. It is possible to calibrate the SCrE at a low concentration of such an electrolyte, and then to use this information at higher concentrations, and even for other electrolytes. However, this is not necessarily a safe procedure. Analysis of surface reactions and application of SCM,²⁰ leads to the conclusion that at higher ionic strengths the values of pH_{pzc} and pH_{iep} are shifted from the pH_{eln} , but in the opposite direction. In the case of preferential association of cations ($K_{\text{C}}^{\circ} > K_{\text{A}}^{\circ}$): $\text{pH}_{\text{pzc}} < \text{pH}_{\text{eln}} < \text{pH}_{\text{iep}}$. Contrary, in the case of preferential association of anions ($K_{\text{A}}^{\circ} > K_{\text{C}}^{\circ}$): $\text{pH}_{\text{pzc}} > \text{pH}_{\text{eln}} > \text{pH}_{\text{iep}}$. It has been shown²⁰ that pH_{pzp} lies between pH_{pzc} and pH_{eln} so that the point of zero charge is a better approximation for the location of the point of zero potential with respect to the isoelectric point.

In principle, to obtain the values of the surface potential, one needs to subtract all other contributions, E_{T} , from the measured electrode potentials E

$$\Psi_0 = E - E_{\text{T}} \quad (40)$$

The value of E_{T} includes potential differences at all interfaces such as *e.g.* crystal/mercury, mercury/graphite, graphite/copper, *etc.* Since the value of E_{T} does not depend on the composition of the solution, it suffices to perform calibration just at one condition. It is sufficient to know the condition at which the surface potential is zero *i.e.* pH_{pzc} . In such a case

$$E_{\text{T}} = E_{\text{pzc}} \quad (41)$$

There are several “zero points” related to electrostatic charge and/or potential at the interface:

- the electroneutrality point (eln) characterized by pH_{eln} , determined by the interfacial equilibrium constant (Equation 20). It is also called “pristine point of zero charge”.^{20–35}
- the common intersection point (c.i.p.) characterized by pH_{cip} being a single cross over point of $\sigma_0(\text{pH})$ curves at different ionic strength obtained from acid-base potentiometric titrations (pH which remains constant despite addition of the electrolyte)
- the point of zero charge (p.z.c.) corresponding to zero surface charge in the 0-plane, *i.e.* to $\sigma_0 = 0$, and characterized by pH_{pzc} . It is often approximated by pH_{cip} , despite possible significant discrepancies, which have been reported in the literature.^{7,8,36,48} The more reliable methods for p.z.c. determination are the “mass titration” technique,^{49,50} “pH-shift” method^{51–53} and “electrolyte titration” technique.⁵⁴

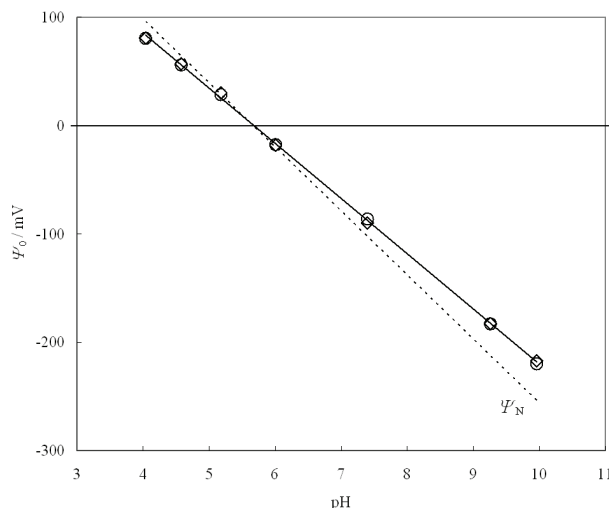


Figure 3. Surface potential (Ψ_0) of rutile (001) plane as a function of pH in aqueous KNO_3 solution ($I_{\text{c}} = 0.001 \text{ mol dm}^{-3}$) at 25 °C. The Nernstian potential (Ψ_{N}) is represented by the dashed line. Surface potential Ψ_0 was obtained from the measured electrode potentials taking into account the isoelectric point for the rutile (001) plane $\text{pH}_{\text{iep}} \approx 5.7$. Reproduced with permission from *Croatica Chemica Acta*.⁴⁵

- the electrokinetic isoelectric point (i.e.p.) corresponding to zero value of the electrokinetic mobility, which usually corresponds to zero ζ -potential, *i.e.* to $\zeta = 0$, and characterized by pH_{iep} .⁷ Several electrokinetic techniques are in use, and sometimes different values of zeta potentials are obtained on the same sample when different techniques are used. The evaluated ζ -potentials may therefore be questionable, but the zero point (zero mobility) can be precisely detected without any assumption for homogeneous particles.
- the point of zero potential (p.z.p.) corresponding to $\Psi_0 = 0$, and characterized by pH_{pzp} . This point cannot be detected directly, but has to be deduced from pH_{pzc} and pH_{iep} .

At low ionic strength, and also in the case of equal affinities of counterions (cations and anions) towards association with oppositely charged surface groups, all “zero points” coincide. Therefore, it is advisable to calibrate SCrE (determine E_{T} value, Equation (40)) by measuring pH_{iep} and pH_{pzc} at low concentration of suitable electrolytes. If these two “zero points” are found to be equal one may take this value as corresponding to the value of zero potential. If such a condition cannot be achieved one may take the intermediate value between pH_{iep} and pH_{pzc} or exclusively the point of zero charge as approximation for the point of zero potential.²⁰ However, in most cases the difference is not too significant and one may use the isoelectric point as the point of zero potential. Figure 3 presents an example of surface potential measurements using the rutile single crystal electrode.

The measurements of the surface potential by electrodes with single crystals open the possibility of analyzing different crystal planes. It is commonly accepted that different planes, and also edges, exhibit different behavior, *i.e.* different reactions characterized by corresponding specific equilibrium constants. Even a plane will usually involve different active and inactive surface sites of concomitant site densities, which are all characterized with their respective affinities towards binding of potential determining ions and association of counter ions from the bulk of the solution. An example is given in Figure 4 for the 110 cut of goethite (α -FeOOH). Nominally three different sites exist on this plane (*i.e.* singly, doubly and triply coordinated groups). Due to the presence of two structurally different iron atoms in goethite, two kinds of triply coordinated groups can be distinguished, one having a strong affinity for protons, $\text{Fe}_3\text{O}_1\text{H}$, and another having weak proton affinity, *i.e.* preferring H-bond acceptance, $\text{Fe}_3\text{O}_{1\text{I}}$. Within this model, which is based on Hiemstra *et al.*,⁵⁸ these two sites as well as the doubly coordinated groups do not exhibit pH dependent behavior over the usual pH range. Based on the simple bond-valence principle the charge on these groups corresponds to the numbers in Figure 4a. These groups contribute charges to the overall surface charge. On this surface the formalism of the 1-pK, 2-pK concepts are combined, both in terms of the fractional charges and in terms of the protonation steps.

The protonation of the doubly coordinated group corresponds to that in the classical two-step (*i.e.* 2-pK) mechanism. The triply coordinated groups can only exist in two states (protonated or deprotonated) and therefore correspond to a true one-step (*i.e.* 1-pK) mechanism.

The only group that exhibits pH-dependent behaviour is the singly coordinated group. It has a value of the thermodynamic (intrinsic) equilibrium constant for the deprotonation of the $\text{FeOH}_2^{+1/2}$ species of about $\text{p}K = -\log K = 8$. This intrinsic $\text{p}K$ value is shifted to the apparent value of about 3 by the electrostatic terms. This difference of about 5 pH units (!) is enormous and it would indicate that even if the speciation of one surface group could be determined as a function of pH by spectroscopy, it would NOT yield the intrinsic $\text{p}K$ value for the group, if other groups are present. Within the typical pH range the singly coordinated groups display a one-step (*i.e.* 1-pK) behaviour. The deprotonation of the hydroxo group to form the oxo group according to the model would occur at pH values which are typically not studied. In the same line of reasoning the occurrence of the μ -aquo and μ -oxo groups is not expected in the pH range considered. For the triply coordinated groups again only one respective group predominates. Protonation or deprotonation of these groups would occur at very low or very high pH. The resulting point of zero charge of this plane is about 9.4, which is in close

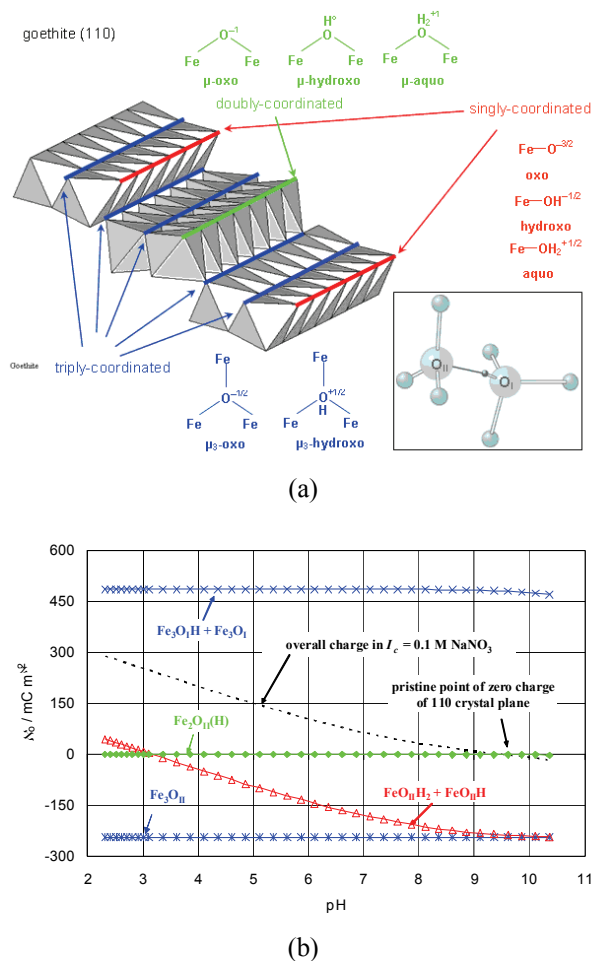


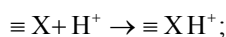
Figure 4. Structure of the 110 plane of the goethite (a) and charge of the 110 plane and the contributions from the various surface groups (b).

agreement with experimental data on goethite samples, where the 110 plane is expected to dominate.

The groups are subject to a common, smeared out (inner) surface potential. To each of the groups bearing a charge, association of counter-ions may occur. Usually association constants to each of the different groups could be different, but it is impossible to distinguish that detail based on experimental data. It might be possible to obtain the information from future advanced theoretical work. The example from Figure 4 displays the potential complexity for just one crystal plane with various surface sites.

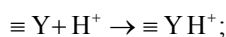
If only one plane with only one kind of surface site is exposed to the liquid medium the situation becomes relatively simple. This is the case for the basal plane of sapphire or hematite. However, if two or more different planes with different surface sites are exposed to the liquid medium not only there will be several groups, also the interfacial reactions are mutually influenced by the common (inner) surface potential. As stated by Yanina and Rosso, the important parameter in

mutual influence of different crystal planes at mineral/aqueous solution interfaces is the crystal conduction.⁵⁹ Let us consider two crystal planes; one with surface sites $\equiv X$ and the other with surface sites $\equiv Y$ that have different affinities towards association with protons, characterized by different equilibrium constants. If the individual planes are exposed to the aqueous electrolyte solution, the surface potentials of these two may be different. According to the SCM



$$K_X^\circ = \exp(F\Psi_0 / RT) \cdot \frac{\{\equiv XH^+\}}{\{\equiv X\} \cdot a_{H^+}} \quad (42)$$

$$\Psi_0 = \frac{RT \ln 10}{F} \log K_X^\circ - \frac{RT \ln 10}{F} \log \left(\frac{\{\equiv XH^+\}}{\{\equiv X\}} \right) - \frac{RT \ln 10}{F} \text{pH} \quad (43)$$



$$K_Y^\circ = \exp(F\Psi_0 / RT) \cdot \frac{\{\equiv YH^+\}}{\{\equiv Y\} \cdot a_{H^+}} \quad (44)$$

$$\Psi_0 = \frac{RT \ln 10}{F} \log K_Y^\circ - \frac{RT \ln 10}{F} \log \left(\frac{\{\equiv YH^+\}}{\{\equiv Y\}} \right) - \frac{RT \ln 10}{F} \text{pH} \quad (45)$$

However, if these two planes are in contact with the electrolyte solution at the same time, due to the conduction within the crystal, both planes will have the same potential, *i.e.* the charged surface groups $\equiv XH^+$ and $\equiv YH^+$ will be exposed to the same (common) potential Ψ_0 . The value of the common potential will lie between individual potentials characterized by reactions (42,44), *e.g.* between potentials that would be measured if individual planes are exposed to the liquid medium separately. By adding Equations (43,45) one obtains

$$\Psi_0 = \frac{RT \ln 10}{2F} \log(K_X^\circ \cdot K_Y^\circ) - \frac{RT \ln 10}{F} \log \left(\frac{\{\equiv XH^+\} \cdot \{\equiv YH^+\}}{\{\equiv X\} \cdot \{\equiv Y\}} \right) - \frac{RT \ln 10}{2F} \text{pH} \quad (46)$$

while the subtraction yields the ratio of thermodynamic equilibrium constants

$$\frac{K_X^\circ}{K_Y^\circ} = \frac{\{\equiv XH^+\} \cdot \{\equiv Y\}}{\{\equiv YH^+\} \cdot \{\equiv X\}} \quad (47)$$

However, it may happen that due to kinetic effects one of the crystal planes prevails in equilibration so that a common potential will be closer to the individual potential of this “more powerful” plane. The common potential could be still a linear function of pH with the slope significantly lower than the Nernstian. Surface potential measurements may be helpful in analyzing such phenomena. The above analysis is also related to real systems of crystals exposing different planes to the solution at the same time. This analysis also pertains to single planes with surface sites of different affinities towards protons.

The outer surface potential Ψ_β

The state of associated counterions is affected by outer surface potential Ψ_β which is not a measurable quantity, but could be obtained by considering equilibrium in the EIL. This potential could be calculated from measured inner surface potentials Ψ_0 and corresponding surface charge densities in the 0-plane σ_0 if the inner layer capacitance C_1 is known. According to Equation (25)

$$\Psi_\beta = \Psi_0 - \frac{\sigma_0}{C_1} \quad (48)$$

The outer layer potential could be also deduced from the potential at the onset of the diffuse layer being according to Equation (26,27)

$$\Psi_\beta = \Psi_d + \frac{\sigma_s}{C_2} = \Psi_d + \frac{\sqrt{8RT\varepsilon I_c} \sinh(-F\Psi_d / RT)}{C_2} \quad (49)$$

It should be noted that according to the BSM approximation the diffuse layer extends from the β -plane (β - and d -planes are identical) so that the outer surface potential Ψ_β is equal to the potential at the onset of diffuse layer Ψ_d . The charge density in this plane can be experimentally estimated by measuring the adsorption of counter-ions. However, the measurements will also involve diffuse layer contributions. Definitively characterization of this plane is currently a model issue.

The diffuse layer potential Ψ_d

The diffuse layer potential Ψ_d , or more precisely the potential at the onset of the diffuse layer, determines ionic distribution within the diffuse layer. According to the Gouy–Chapman theory the potential decreases from the original value Ψ_d to zero in the bulk of the solution. The extension of the diffuse layer is represented by the Debye–Hückel distance $l_{DH} = \kappa^{-1}$ (Equation (32)), but it should be noted that at the distance l_{DH} the electrostatic potential is still significant.

The diffuse layer potential is useful in calculations of the net surface charge density σ_s (Equation (27)).

Also, it plays the essential role in controlling the stability of colloidal systems.⁶⁰ In the course of the collision of two particles a partial overlap of two diffuse layers takes place. Since the charge distribution within diffuse layers is determined by Ψ_d it is obvious that this quantity is responsible for the energy barrier and the rate of the aggregation of particles.

As all other potentials within the EIL, the diffuse layer potential could be obtained for a given condition if the mechanisms of surface reactions were known, as well as the values of the corresponding equilibrium parameters. The value of Ψ_d could be calculated from the measured electrokinetic potential by means of the Gouy-Chapman theory (Equation (30)). For that purpose the slip plane separation distance should be known. Broadman and Eversole,⁶¹ suggested that the slip plane separation may be obtained from the dependency of the electrokinetic ζ -potential on the ionic strength *via* Gouy-Chapman theory. Accordingly, the slip plane separation may be obtained from a linear plot (Equation (31)). However, such a procedure assumes a constant Ψ_d potential at variable activity of potential determining ions (constant pH for metal oxides) which is not the case. At higher ionic strengths the Ψ_d value decreases due to more pronounced counterion association so that function in Equation (47) is not linear and the slope at a certain ionic strength is higher than l_e . Therefore by using this method one may find that l_e is lower than *e.g.* 5 nm, but cannot obtain the proper value. Another more complicated route is to use Equations (25,26) and to calculate Ψ_d from measured inner surface potential data. However, for that purpose the values of surface charge densities and capacitances should be known.

The potential at the onset of the diffuse layer Ψ_d can be inferred from Atomic Force Microscopy (AFM) data.²⁶ Coagulation (aggregation) and adhesion experiments may provide information on the condition at which $\Psi_d = 0$ which in most cases correspond to the isoelectric point.^{62,63}

The electrokinetic potential ζ

The electrokinetic potential, often called ζ -potential, is assumed to occur at the hypothetical slip (or shear) plane that divides the stagnant from the mobile part of the diffuse layer. Its separation from the d-plane is of the order of one nanometer. For aqueous systems the value of $l_e = 1.5$ nm was found to be representative.⁶⁴ The primary significance of electrokinetic methods is that they provide information on the sign of the net surface charge and on the isoelectric point. There are several commercially available techniques developed for electrokinetic measurements, such as electrophoresis, acoustophoresis, streaming potential and streaming current. The evaluation of the ζ -potentials from measured data (such as mobility in the case of electrophore-

sis) and the problems associated with the evaluation is the subject of numerous research articles and review papers^{5,7,25,65} so that it will not be discussed here. The significance of the ζ -potential lies in the possibility of experimental evaluation and the fact that its value is close to (but still little lower in magnitude than) the potential at the onset of the diffuse layer which could be obtained on the basis of Equation (30). On a semi quantitative basis the electrokinetic data, such as sign of charge and isoelectric point, may serve to predict the behavior of the system. For example, negatively charged organic molecules would get adsorbed to positively charged surface, positively charged colloid particles would adhere to negatively charged surfaces, *etc.*

SOME REMARKS ON DIFFUSE LAYER POTENTIALS OF REAL SOLID/ELECTROLYTE SOLUTION INTERFACES

In previous paragraphs the models of plane electric interfacial layer (EIL) were discussed. In Figure 1, the schematic representation of the EIL is shown in which four planes and four layers are distinguished. The models consider completely flat solid surface (zero plane) on which excess positive or negative electric charge exists resulting from the surface reactions. In case of solid oxides and hydroxides the reactions involve H^+ and OH^- potential determining ions. These surface charges attract electrostatically (in some systems also chemical interactions may occur) the counterions that partially compensate the surface charge thus forming the stagnant part of the EIL. The rest of the EIL has diffuse character (see Figure 1), however one can ask how thick is the EIL. From a thermodynamic point of view it ends in the bulk solutions where the chemical potentials of the coions and counterions do not change with the distance from the zero plane, or in other words; where the electric potential drops to zero relative to the bulk solution. However, it is more illustrative to express the thickness in metric scale, *i.e.* nanometers. The effective thickness of the diffuse part can be easily calculated from Debye-Hückel parameter $l_{DH} = 1/\kappa$, which is determined by the temperature and effective permittivity and also by the ionic strength of the electrolyte, *i.e.* by concentrations and charges of the ions. According to Equation (32), for aqueous solutions at 25 °C, $\kappa/nm^{-1} = 3.288 \times (I_c/mol\ dm^{-3})^{1/2}$.

Table 1 shows the diffuse layer thickness in commonly applied electrolytes. While in 0.1 mol dm^{-3} NaCl its thickness is only about 1 nm, *i.e.* about 3 dimensions of water molecules, in 10^{-5} mol dm^{-3} NaCl solution it ranges up to almost 100 nm and even tenfold more in pure water, at least using the above relationship. It should be stressed that $1/\kappa$ is an effective thickness and the potential drop extends up to $3/\kappa$, where 98 % of the initial Ψ_d potential value drops away.⁵⁵ However, this

parameter ($1/\kappa$) is based on the assumption of dimensionless ions and structureless solvent.

The whole EIL (including the stagnant layer) is obviously thicker than the diffuse part by the distance d being at least dimension of one partially hydrated counterion and possibly one hydrated layer of the ions (Figure 1). For example, the ionic radius of Na^+ (in a 6 coordinated crystal lattice) is 1.02 Å, while its hydrated radius is 2.18 Å.^{66,67} In the case of K^+ the values are 1.38 Å and 2.12 Å, and for Mg^{2+} the radii are 0.72 Å and 2.99 Å, respectively.⁶⁷ Of course, later on, after Gouy and Chapman derived their model of the electrical double layer, many advanced models have been elaborated in which solvent structure and interaction between the ions and solvent, modification of the Poisson-Boltzmann Equation, integral Equation theory, cluster expansion theory, and others, were taken into account.⁶⁸ As an example we refer to Bohinc *et al.*⁶⁸ By applying statistical mechanics the authors have proposed a model of flat electrical interfacial layer thickness in which the ion sizes were included. In the calculation the electrostatic mean field and the effect of excluded volume was considered. In the Bohinc model the ions are distributed in the solution over a lattice and their different sizes are expressed by values of the lattice constant. The authors upgraded Poisson-Boltzmann (P-B) distribution theory, by considering the finite size of ions. However, their calculations were limited to electrolytes, in which the anions and cations are of equal size. The model results showed that the effective thickness of the EIL increases with increasing ion size, which is several nanometers for large counterions having the size of 1 nm. In case of small values of the lattice constant the results approach those from classical Poisson-Boltzmann Equation. With the increase in the surface charge density σ_s , the effective thickness of EIL containing counterions decreases, reaches a minimum and then increases. Next to the charged surface the counterion density is markedly determined by their size (the lattice constant) and this dependence weakens with increasing distance from the zero plane (Figure 1). With the help of spectroscopic methods it was confirmed that counterions are indeed present at high concentration at the charged surface and then their concentration sharply decreases as the distance from the 0-plane increases.⁶⁷ Bohinc *et al.*⁶⁸ concluded that the Debye-Hückel length should be used with caution, especially in the case of large ions and highly charged surfaces.

The EIL can be considered as flat if the surface potential Ψ varies only along the normal direction from the solid surface, *e.g.* $\partial\Psi/\partial x$, while $\partial\Psi/\partial y = \partial\Psi/\partial z = 0$. This condition is fulfilled for flat surfaces and for large particles, *i.e.* if $\kappa a \gg 1$, where a denotes the radius of the curvature (particle). In practice the requirement is that $\kappa a > 100$.⁵⁵ In such a case, in 0.1 mol dm⁻³ of 1:1 aqueous electrolyte at 298 K, $\kappa = 1.040 \text{ nm}^{-1}$, and the

Table 1. Effective thickness of the diffuse part, l_{DH} , of the EIL for aqueous solutions at 25 °C as a function of electrolyte concentration, calculated using Equation (32)

Aqueous solution	$c / \text{mol dm}^{-3}$	$l_{\text{DH}} / \text{nm}$
Pure water (pH = 7)	0	961.8
NaCl	10^{-5}	96.2
NaCl	10^{-3}	9.6
NaCl	10^{-2}	3.0
NaCl	10^{-1}	0.96
Na_2SO_4	10^{-5}	60.8
Na_2SO_4	10^{-3}	6.1
Na_2SO_4	10^{-1}	0.61
MgSO_4	10^{-5}	48.1
MgSO_4	10^{-3}	4.8
MgSO_4	10^{-1}	0.48

particle radius a should be above 100 nm. However in 0.001 mol dm⁻³ electrolyte, $\kappa = 0.104 \text{ nm}^{-1}$ and the particle radius should be above 1000 nm. These simple calculations clearly show that in more concentrated electrolytes (0.1 mol dm⁻³) the electrical interfacial layer can be already considered as a flat one if the particle radius is above 100 nm, but in 0.001 mol dm⁻³ electrolyte solution the minimal particle radius has to be close to 1 μm or larger. The derivations for spherical double layer are more complicated. They can be found, for example, in Wang *et al.*,⁷⁰ who used an iterative method in functional analysis to solve the Poisson-Boltzmann Equation (see also Equation (34)). Generally, the thickness of spherical double layers is related to the distribution of the space charge, and the authors considered the problem as an imaginary capacitor with the distance between the shells equivalent to the thickness of the EIL. These issues are not, however, a subject of this article.

To study experimentally the electrochemical properties at the oxide/electrolyte solution interface *via* surface charge determination (potentiometric titration) and/or electrokinetic measurements, the samples should possess relatively large specific surface area (at least 10 m²/g) which requires a suspension of small particles. Accordingly in the interpretation of the experimental data we are “balancing on the border” of flat *vs.* curved electrical interfacial layer. However, even if the particles are large enough to fulfill the condition of a flat layer, the question is what is the local flatness (or curvature) of such particles. The sophisticated advanced methods that are now developed (*e.g.* Scanning Electron Microscopy, Atomic Force Microscopy) allow for insight into solid/electrolyte solution interfaces on molecular level. On this level it is hardly possible to obtain a really flat oxide/electrolyte interface for commonly available samples of a larger size, and the experimental

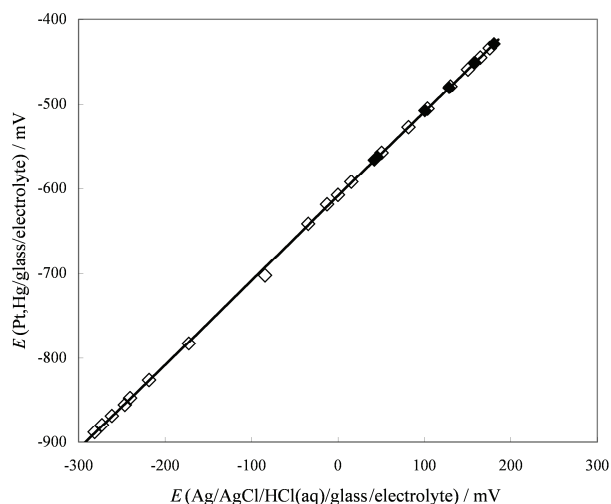


Figure 5. The relationship between potentials of the glass electrode filled with mercury and ordinary glass electrode filled with HCl. Titration with HNO_3 (full symbols) and retitration with KOH (open symbols). The straight line represents the slope equal to 1.

results represent, in the best case, some apparent averaged plane EIL consisting of many micro-planes. However, it is difficult to judge whether we can treat such an interface as a flat or curved (spherical) one. This is not important in the surface charge determination by potentiometric acid-base titration, but it is important in the interpretation of the electrokinetic phenomena. On the other hand, determination of electrical properties (surface and electrokinetic potential) for single crystals of well known planes orientation might be an alternative to gain knowledge about real solid surface/electrolyte solution interface state.

GLASS ELECTRODE

According to the results obtained with Single Crystal Electrodes and to the theory based on the Surface Complexation Model, one may conclude that the response of glass electrodes used for pH measurements is the result of binding to and release of H_3O^+ and OH^- ions from the glass surface. The commercial glass electrode is filled with HCl solution so that potential difference occurs both at inner and outer interfaces. The developed potential difference at the inner surface is constant, while at outer surface it depends on the pH of the examined solution. But, the speculation based on diffusion of H_3O^+ and OH^- ions through glass, and the concept of pH dependent diffusion potential, or ion exchange mechanism, cannot be simply disregarded. In order to prove that surface complexation involving H_3O^+ and OH^- ions is responsible for the response of the glass electrode, the following experiments were performed.⁷¹

Two commercial glass electrodes (Iskra, Kranj) were employed. Both of them were calibrated with buffers at 25 °C and showed the slope of -58.1 mV, which is 98 % of the Nernstian slope. Then, one electrode was cut at the top, the Ag/AgCl wire was taken off, the HCl solution was discharged, and the inside of the electrode was rinsed with water and dried. In the second step the electrode was filled with mercury and the contact was ensured with platinum wire. Titration was performed by addition of HNO_3 and the retitration with KOH. The same saturated calomel electrodes were used for measurements of the potential of both electrodes. The results are presented in Figure 5. From this experience it could be concluded, that the glass electrode filled with mercury had the same response as the glass electrode filled with aqueous HCl solution. The only difference lies in the standard potential. The slope of the glass electrode filled with mercury, which is similar to Single Crystal Electrodes, is 98 % with respect to the Nernst Equation. Experiments were repeated in 1 mol dm^{-3} KNO_3 and NaNO_3 and showed the same behavior.

Similar experiments were performed with the electrode made of common laboratory glass. However, in this case the slope was significantly lower *i.e.* 80 % with respect to Nernstian behavior.

According to the above experiments one may conclude that glass electrodes exhibit essentially the same mechanism as metal oxide Single Crystal Electrodes. Their slope should be lower with respect to the prediction based on the Nernst Equation. The composition of glass used for commercial electrodes is adjusted so that the slope is almost equal or very close to the Nernstian slope and the conductivity of the glass should be as low as possible.

It should be noted that the first glass electrode with direct metal connection was constructed by Thompson⁷² in 1932 but did not show the proper response, probably due to pure contact between glass and metal. This was improved in our laboratory in 1985 by using mercury⁷¹ and published⁷³ in 1990. Cheng and Ashraf published the paper⁷⁴ on solid-state pH glass electrode with conductive silver paste ensuring proper electrical contact with the inner dry glass surface. These results enabled Cheng to postulate the “non-faradaic” mechanism of the glass electrode function⁷⁵ for which a more proper name would be “ionic adsorption” mechanism.

CONCLUSION

Electrostatic potentials within the Electrical Interfacial Layer (EIL) at solid/liquid interfaces are the result of ionic distribution, which is influenced on the other hand by the potential. Therefore, evaluation of the potentials of characteristic planes within EIL provides significant

information on the interfacial equilibrium. A full characterization of one surface such as a defined cut of a single crystal yielding all the different properties discussed above is still missing. This is due to the fact that, for example, proton adsorption experiments cannot be carried out using single crystals (the surface area being too small for potentiometric titrations, grinding the samples to increase the surface area is not possible since it will make fresh surfaces with different reactivities). One might think of studying electrolyte adsorption (*i.e.* counterion adsorption) to such single crystals using radioactive tracers or non-linear optic techniques.⁷⁶ This would constrain the association constants. Surface potential and streaming current measurements will yield well defined values for the (relative) inner-surface potential and the zeta-potential. For well-defined colloidal particles surface potential measurements are not straightforward, and zeta-potentials will involve assumptions. In this case potentiometric titrations and counter-ion adsorption can be studied more easily.

Presently, comprehensive approaches do not involve all possible measurements on one sample, but this will be possible in the future. It is expected that this might result in some surprises (such as the already observed binding of nitrate to negatively charged silica surfaces),⁷⁶ but ultimately it will be possible to constrain the parametrisation of surface complexation models in a much more vigorous way than today.

Acknowledgements. This work was partially supported by the Ministry of Science, Education and Sports of the Republic of Croatia (project 119-1191342-2961). Support from within the European project ACTINET is also acknowledged.

REFERENCES

- N. Kallay, D. Kovačević, and A. Čop, *Interpretation of Interfacial Equilibria on the Basis of Adsorption and Electrokinetic Data*, in: N. Kallay (Ed.) *Interfacial Dynamics*, Marcel Dekker, Inc., New York, 2000.
- N. Kallay, S. Žalac, and D. Kovačević, *Thermodynamics of the Solid/Liquid Interface. Its Application to Adsorption and Colloid Stability*, in: J. Lützenkirchen (Ed.), *Surface Complexation Modelling*, Interface Science and Technology series, Elsevier, 2006.
- D. E. Yates, S. Levine, and T. W. Healy, *J. Chem. Soc. Faraday Trans. 1* **70** (1974) 1807–1818.
- W. Stumm, C. P. Huang, and S. R. Jenkins, *Croat. Chem. Acta* **42** (1970) 223–245.
- A. V. Delgado, F. Gonzalez-Caballero, R. J. Hunter, L. K. Koopal, and J. Lyklema, *Pure Appl. Chem.* **77** (2005) 1753–1805.
- H. Ohshima, *Diffuse Double Layer Equations for Use in Surface Complexation Models: Approximations and limits*, in: J. Lützenkirchen (Ed.), *Surface Complexation Modelling*, Interface Science and Technology series, Elsevier, 2006.
- H. Lyklema, *Fundamentals of Interface and Colloid Science*, Volume II: *Solid-Liquid Interface*, Academic Press, London, 1995.
- D. Kovačević, T. Preočanin, and S. Žalac, A. Čop, *Croat. Chem. Acta* **80** (2007) 287–301.
- J. F. Schnecko, *J. Colloid Interface Sci.* **61** (1977) 569–576.
- C. Chicos and T.H. Geidel, *Colloid Polym. Sci.* **261** (1983) 947.
- L. Bousse, N.F. De Rooij, and P. Bergveld, *Surf. Sci.* **135** (1983) 479.
- S. Ardzzone and S. Trasatti, *J. Electroanal. Chem.* **126** (1981) 287–292.
- S. Ardzzone and M. Radaelli, *J. Electroanal. Chem.* **269** (1989) 461–469.
- M. J. Avena, O. R. Camara, and C. P. De Pauli, *Colloids Surf.* **69** (1993) 217–228.
- N. G. H. Penners, L. K. Koopal, and J. Lyklema, *Colloids Surf.* **21** (1986) 457–468.
- E. Kinoshita, F. Ingman, and G. Edwall, *Electrochim. Acta* **31** (1986) 29–38.
- N. Kallay and D. Čakara, *J. Colloid Interface Sci.* **232** (2000) 81–85.
- N. Kallay, A. Čop, E. Chibowski, and L. Holysz, *J. Colloid Interface Sci.* **259** (2003) 89–96.
- N. Kallay, Z. Dojnović, and A. Čop, *J. Colloid Interface Sci.* **286** (2005) 610–614.
- N. Kallay, T. Preočanin, and T. Ivšić, *J. Colloid Interface Sci.* **309** (2007) 21–27.
- T. Preočanin, A. Čop, and N. Kallay, *J. Colloid Interface Sci.* **299** (2006) 772–776.
- T. Preočanin, W. Janusz, and N. Kallay, *Colloids Surf. A* **297** (2007) 30–37.
- T. Preočanin, M. Tuksar, and N. Kallay, *Applied Surf. Sci.* **253** (2007) 5797–5801.
- N. Kallay, T. Preočanin, J. Marković, and D. Kovačević, *Colloids Surf. A* **306** (2007) 40–48.
- A. S. Dukhin and P. J. Goetz, *Ultrasound for Characterizing Colloids, Particle Sizing, Zeta Potential, Rheology*, Elsevier, Amsterdam, The Netherlands, 2002.
- X. Yin and J. Drelich, *Langmuir* **24** (2008) 8013–8020.
- W. H. van Riemsdijk, G. H. Bolt, L. K. Koopal, and J. Blaakmeer, *J. Colloid Interface Sci.* **109** (1986) 219–228.
- R. H. Yoon, T. Salma, and G. Donnay, *J. Colloid Interface Sci.* **70** (1979) 483–493.
- T. Hiemstra, P. Venema, and W. H. van Riemsdijk, *J. Colloid Interface Sci.* **184** (1996) 680–692.
- N. Kallay, T. Preočanin, and S. Žalac, *Langmuir* **20** (2004) 2986–2988.
- J. A. Davis, R. O. James, and J. O. Leckie, *J. Colloid Interface Sci.* **63** (1978) 480–499.
- W. Rudzinski, R. Charmas, W. Piasecki, J. M. Cases, M. Francois, F. Villieras, and L. J. Michot, *Colloids Surf. A* **137** (1998) 56–87.
- M. A. Pyman, J. W. Bowden, and A. M. Posner, *Aust. J. Soil Res.* **17** (1979) 191.
- J. Lyklema, *J. Colloid Interface Sci.* **99** (1984) 109.
- J. Sonnefeld, *Colloids Surf. A* **190** (2001) 179.
- G. Sposito, *Environ. Sci. Technol.* **32** (1998) 2815–2819.
- D. A. Sverjensky, *Geochim. Cosmochim. Acta* **65** (2001) 3643–3655.
- E. F. de Souza, G. Ceotto, and O. Teschke, *J. Mol. Catalysis A* **167** (2001) 235–243.
- J. O'M. Bockris, A. K. N. Reddy, M. Gamboa-Aldeco, in: *Modern Electrochemistry: Fundamentals of Electrode Processes*, Chapter 6., Vol 2A, Kluwer, New York, 2002. pp.771–1033.
- J. Lützenkirchen, J. F. Boily, L. Lovgren, and S. Sjöberg, *Geochim. Cosmochim. Acta* **66** (2002) 3389–3396.
- T. Preočanin and N. Kallay, *Croat. Chem. Acta* **71** (1998) 1117–1125.
- R. O. James and G. A. Parks, *Characterization of Aqueous Colloids by their Electrical Double-Layer and Intrinsic Surface Chemical Properties*, in: E. Matijević (Ed.), *Surface and Colloid Science*, Vol. 12, Plenum Press, New York, London, 1982, pp 119–216.
- A. Fujishima and K. Honda, *Nature* **238** (1972) 37–38.

44. R. K. Quinn, R. D. Nasby, and R. J. Baughman, *Mat. Res. Bull.* **11** (1976) 1011–1018.
45. N. Kallay, T. Preočanin, A. Selmani, F. Šupljika, and I. Leniček, *Croat. Chem. Acta* **82** (2009) 323–327.
46. V. Simeon, *Chem. Int.* **26** (2004) 18.
47. N. Kallay, A. Čop, T. Preočanin, and D. Kovačević, *Annales UMCS Sectio AA* **60** (2005) 47.
48. J. Lützenkirchen and P. Magnico, *Colloids Surf. A* **137** (1998) 345–354.
49. J. S. Noh and J. A. Schwarz, *J. Colloid Interface Sci.* **130** (1989) 157–164.
50. S. Žalac and N. Kallay, *J. Colloid Interface Sci.* **149** (1992) 233–240.
51. S. K. Milonjić, A. Lj. Ruvarac, and M. V. Šušić, *Thermochim. Acta* **11** (1975) 261–266.
52. J. J. Gulicovski, Lj. S. Čerović, and S. K. Milonjić, *Materials and Manufacturing Processes* **23** (2008) 615–619.
53. K. Bourikas, C. Kordulis, and A. Courghiotis, *Environ. Sci. Technol.* **39** (2005) 4100–4108.
54. T. Preočanin and N. Kallay, *Croat. Chem. Acta* **79** (2006) 95–106.
55. R. J. Hunter, *Zeta Potential in: Colloid Science*, Academic Press, London, 1981.
56. A. S. Dunkin and P. J. Goetz, *Ultrasound for Characterizing Colloids, Particle Sizing, Zeta Potential, Rheology*, Elsevier, Amsterdam, The Netherlands, 2002.
57. J. W. Bullard and M. J. Cima, *Langmuir* **22** (2006) 10264–10271.
58. T. Hiemstra, P. Venema, and W.H. Van Riemsdijk, *J. Colloid Interface Sci.* **184** (1996) 680–692.
59. S. V. Yanina and K. M. Rosso, *Science* **320** (2008) 218–222.
60. N. Kallay and S. Žalac, *Croat. Chem. Acta* **74** (2001) 479–497.
61. W. G. Eversole and P. H. Lahr, *J. Chem. Phys.* **9** (1941) 530–534.
62. N. Kallay, Ž. Torbić, M. Golić, and E. Matijević, *J. Phys. Chem.* **95** (1991) 7028–7032.
63. J. Biščan, N. Kallay, and T. Smolić, *Colloids Surf. A* **165** (2000) 115–123.
64. D. Kovačević, N. Kallay, I. Antol, A. Pohlmeier, H. Lewandowski, and H.-D. Narres, *Colloids Surf. A* **140** (1998) 261–267.
65. J. Lyklema, *Colloids Surf. A* **222** (2003) 5–14.
66. Y. Marcus, *Biophysical Chem.* **51** (1994) 111–127.
67. R. D. Shannon, *Acta Cryst.* **32** (1976) 751–767.
68. K. Bohinc, V. Kralj-Iglič, and A. Iglič, *Electrochim. Acta* **46** (2001) 3033–3040.
69. N. Cuvillier, F. Rondelez, *Thin Solid Films* **327–329** (1998) 19–23.
70. Z.-W. Wang, X.-Z. Yi, G.-Z. Li, D.-R. Guan, and A.J. Lou, *Chem. Phys.* **274** (2001) 57–69.
71. V. Starašinić (supervisor N. Kallay), Diploma Thesis, Faculty of Science, University of Zagreb, Zagreb 1985.
72. R. Thompson, *Bur. Stds, J. Research* **9** (1932) 833.
73. N. Kallay, R. Sprycha, M. Tomić, S. Žalac, and Ž. Torbić, *Croat. Chem. Acta* **63** (1990) 467–487.
74. K. L. Cheng and N. Ashraf, *Talanta* **37** (1990) 659.
75. K. L. Cheng, *Microchemical Journal* **72** (2002) 269–276.
76. P. L. Hayes, J. N. Malin, C. T. Konek, and F. M. Geiger, *J. Phys. Chem. A* **112** (2008) 660–668.

SAŽETAK

Elektrostatski potencijali na granici krute i tekuće faze

Nikola Kallay,^a Tajana Preočanin,^a Davor Kovačević,^a Johannes Lützenkirchen^b
i Emil Chibowski^c

^aZavod za fizikalnu kemiju, Kemijski odsjek, Prirodoslovno-matematički fakultet,
Sveučilište u Zagrebu, Horvatovac 102a, 10000 Zagreb, Hrvatska

^bInstitut für Nukleare Entsorgung, Karlsruher Institut für Technologie, Postfach 3640, 76021
Karlsruhe, Germany

^cPhysical Chemistry Department, Faculty of Chemistry, Maria Curie-Skłodowska University,
pl. Marii Curie-Skłodowskiej 3, 20.031 Lublin, Poland

U ovom preglednom članku opisani su elektrostatski potencijali na granici krute faze i elektrolita. Elektrostatski potencijali nekolicine ravnina definirani su i raspravljani: potencijal ispod površine koji utječe na stanje nabijenih vrsta na površini zbog interakcija s potencijal-određujućim ionima (Ψ_0), potencijal koji utječe na stanje asociiranih protiona (Ψ_β), potencijal na početku difuznog sloja (Ψ_d) i elektrokinetički potencijal (ζ). Također, raspravljena je i važnost nulte vrijednosti potencijala te definirane odgovarajuće točke nultog naboja. Izložene su eksperimentalne metode mjerenja potencijala na međupovršinama. Odnos potencijala i naboja na površinama opisani su na temelju Modela površinskog kompleksiranja. Priloženi su poneki eksperimentalni rezultati.